Supporting Information

An ICT-Based Strategy to Colorimetric and Ratiometric Fluorescence Probe for Hydrogen Sulfide in Living Cells

Fabiao Yu,[†] Peng Li,[‡] Ping Song,[‡] Bingshuai Wang,[‡] Jianzhang Zhao[†] and Keli Han*[†‡]

[†] School of Chemical Engineering, Dalian University of Technology, Dalian, 116024, P. R. China; E-mail: yufabiao@163.com
[‡] State Key Laboratory of Moleclar Reaction Dynamics, Dalian Institute of Chemical Physics, Chinese Academy of Sciences; E-mail: klhan@dicp.ac.cn

Contents:

1. **General Experimental Section**
2. **Synthesis and Characterization of Compounds**
3. **Effect of pH Values**
4. **Brightfield Images of Fig. 4**
5. **Confocal Microscopy Imaging for Subcellular Locations of Cy-N_3 in RAW264.7 Cells**
6. **Colorimetric Determination of H_2S in Water Solution and Fetal Bovine Serum**
7. **Time Dependent H_2S Release Associated with Decomposition of H_2S Donor ADT-OH**
8. **RAW264.7 Cells Intracellular Free Extracts Analysis**
9. **Limit of Detection**
10. **Photophysical Properties and Analysis Performances of H_2S Fluorescent Probes**
11. **Theoretical and Computational Methods**

1. General Experimental Section

Materials: The solution of the probe Cy-N_3 (acetonitrile, 1.0 mM) could be maintained in refrigerator at 4°C. 2-[4-Chloro-7-(1-ethyl-3,3-dimethyl(indolin-2-ylidene)]-3,5-(propane-1,3-diyl)-1,3,5-heptatrien-1-yl)-1-ethyl-3,3-dimethyl-3H-indolium (Cy.7.Cl) was synthesized in our laboratory.[1] NO is generated in form of 3-(Aminopropyl)-1-hydroxy-3-isopropyl-2-oxo-1-triazene (NOC-5, 22μM/ml). $O_2^{\cdot-}$ was created by KO_2. The cell-permeant SYTO-16 green fluorescent nucleic acid stain (SYTO-16 dye) exhibited bright, green fluorescence upon binding to nucleic acids. The regents were purchased from Invitrogen Corporation, and used according to the manufacturer's instructions. All other chemicals were from commercial sources and of analytical reagent grade, unless indicated otherwise. RAW264.7 cells (mouse macrophages cell line) were purchased from the Committee on type Culture Collection of Chinese Academy of Sciences. 10 mM NaHS stock solution in HEPES buffer (40 mM pH 7.4). Ultrapure water was used throughout.

[1] N. Narayanan, G. Patonay, *J. Org. Chem.* **1995**, *60*, 2391 – 2395.

Instruments: Fluorescence spectra were obtained by FluoroMax-4 Spectrofluorometer with a Xenon lamp and 1.0-cm quartz cells. Absorption spectra were measured on Lambda 35 UV-visible spectrophotometer (PerkinElmer). ^1H and ^{13}C NMR spectra were taken on a Bruker spectrometer. The fluorescence images of cells were taken using a LTE confocal laser scanning microscope (Olympus FV1000 confocal laser-scanning microscope) with objective lens (×40). USB600 Ultrasonic Cell Disruptor (650 W, ultrasonic probe 2 mm).

Absorption Analysis: Absorption spectra were obtained with 1.0-cm glass cells. The probe Cy-N_3 (acetonitrile, 0.05 mL, 1.0 mM) was added to a 10.0-mL color comparison tube. After dilution to 10 μM with 40 mM HEPES buffers, then various concentrations H_2S was added. The mixture was equilibrated for 20min before measurement.

Fluorescence Analysis: Fluorescence emission spectra were obtained with a Xenon lamp and 1.0-cm quartz cells. The probe Cy-N_3 (acetonitrile, 0.05 mL, 1.0 mM) was added to a 10.0-mL colorcomparison tube. After dilution to 10 μM with 40 mM HEPES buffers, H_2S was added. The mixture was equilibrated for 20 min before measurement. The fluorescence intensity was measured at $\lambda_{ex=}$ 625 nm, fluorescence acquisition from 610 to 850 nm.

Confocal Imaging: Fluorescent images were acquired on Olympus FV1000 confocal laser-scanning microscope with an objective lens (×40). The excitation wavelength was 635 nm. Cell imaging was carried out after washing cells with fresh complete medium (RPMI-1640+20% FBS, 3×1 mL).

Cell Culture: Murine RAW264.7 macrophage cells (ATCC, USA) were maintained following protocols provided by the American Type Culture Collection. Cells were seeded at a density of 1×10^6 cells mL^{-1} for confocal imaging in RPMI 1640 Medium supplemented with 20% fetal bovine serum (FBS), $NaHCO_3$ (2 g/L), and 1%antibiotics (penicillin/streptomycin, 100 U/ml). Cultures were maintained at 37 °C under a humidified atmosphere containing 5% CO_2. Cultures were maintained at

37 °C under a humidified atmosphere containing 5% CO_2. The cells were subcultured by scraping and seeding on 33 mm coverglass slides according to theinstructions from the manufacturer.

2. Synthesis and Characterization of Compounds

Synthesis of 2-{4-(azido)-7-(1-ethyl-3,3-dimethyl(indolin-2-ylidene)}-3,5-(propane-1,3-diyl)-1,3,5-heptatrien-1-yl)-1-ethyl-3,3-dimethyl-3H-indolium (Cy-N_3): Cy.7.Cl (1.0 g, 1.56 mmol), sodium azide (1.0g, 15.6 mmol) were dissolved in 10 mL of anhydrous DMF in a 25-mL round bottom flask under Ar for 7 h at 40 ^oC.[2] Then the solvent was poured into 100 mL ultrapure water. Then the mixture was extracted by dichloromethane (3×50 mL). The solvent was evaporated on a rotary evaporator until dry. The solid was purified on preparative thin-layer chromatography eluted with ethyl acetate. Yield: 35 %. All above operations are carried out under argon atmosphere within 30 min. ^{1}HNMR (400 MHz, CD_3OD-D_4) δ(ppm): 8.47-8.43 (d, 2H), 7.52-7.27 (m, 8H), 6.30-6.26 (d, 2H), 4.24-4.19 (q, 4H), 2.74 (s, 4H), 1.98-1.40 (m, 20H). ^{13}C NMR (CD_3OD-D_4, 100 MHz) δ(ppm):174.0, 145.7, 143.2, 142.8, 129.9, 128.0, 126.6, 123.5, 112.0, 101.9, 50.7, 49.6, 49.4, 49.2, 49.0, 48.8, 48.5, 48.3 40.4, 28.3, 27.4, 22.1, 12.4. LC-MS (API-ES): *m/z* $C_{34}H_{40}N_5^+$Calcd518.7144, found518.7148.

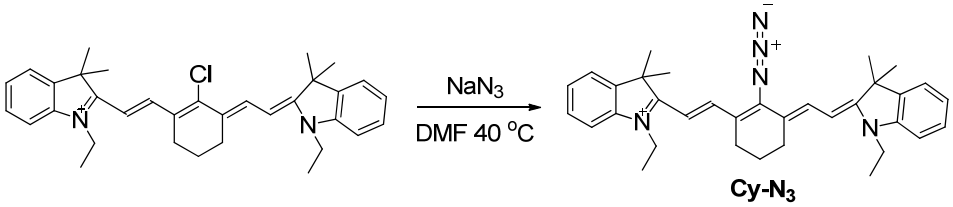

Characterization of 2-{4-amino]-7-(1-ethyl-3,3-dimethyl(indolin-2-ylidene)}-3,5-(propane-1,3-diyl)-1,3,5- heptatrien-1-yl)-1-ethyl-3,3-dimethyl-3H-indolium (Cy-NH_2): Cy-N_3 (0. 1 g, 200 μM) was dissolved in 1 mL acetonitrile. Subsequently, 20 equiv. of NaHS was added. The mixture was equilibrated for 20 min. The solvent was evaporated on a rotary evaporator until dry. The solid was purified on preparative thin-layer chromatography eluted with ethyl acetate. Yield: > 95 %. All above operations are carried out under argon atmosphere. ^{1}HNMR (400 MHz, CD_3OD-D_4) δ(ppm): 8.97-8.83 (d, 2H), 8.05 (s, 2H), 7.52-7.27 (m, 8H), 6.30-6.26 (d, 2H), 5.54 (s, 4H), 4.24-4.19 (q, 4H), 1.20-1.42 (m, 20H). LC-MS (API-ES): *m/z* $C_{34}H_{42}N_3^+$Calcd 492.3373, found [M^+] 492.3330.

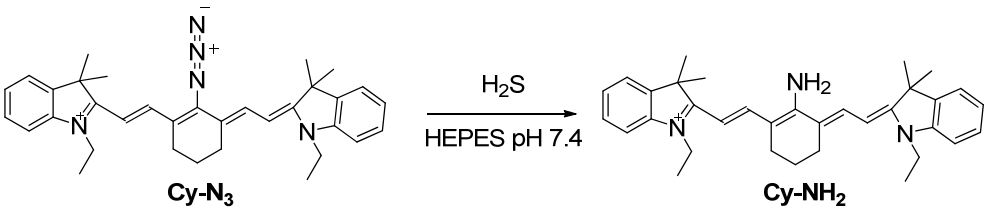

[2] F. Yu, P. Li, G. Li, G.Zhao, T. Chu, K. Han, J. Am. Chem. Soc., 2011, 133, 11030.

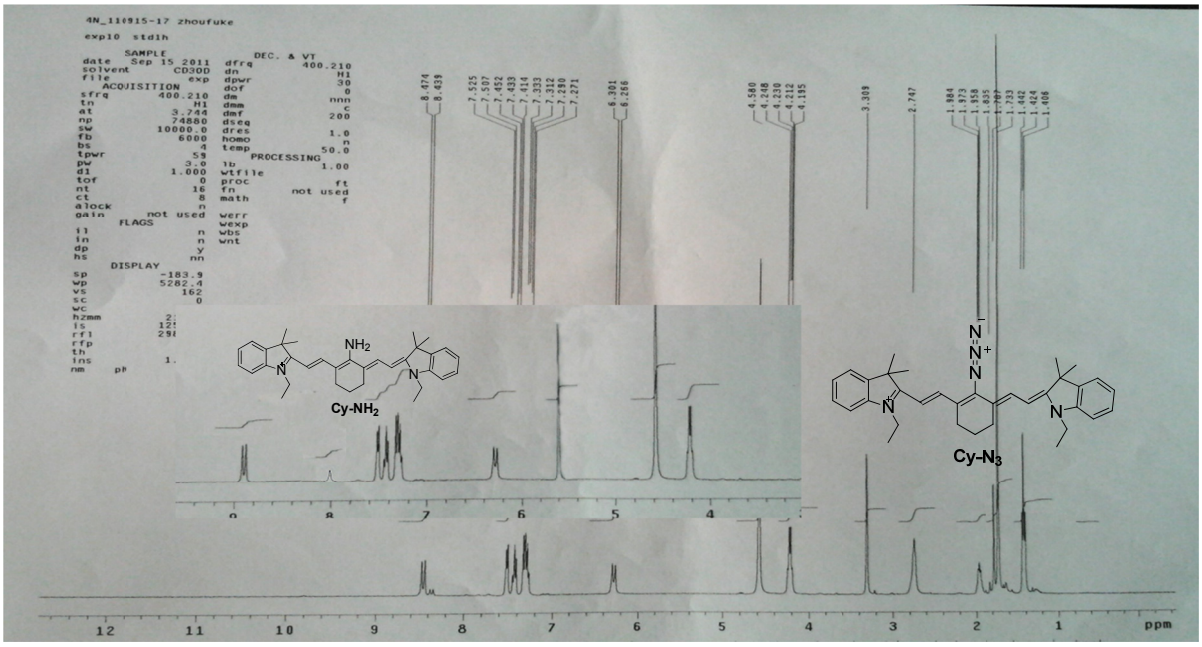

3. Effect of pH Values

The fluorescence intensity might be influenced severely by pH variation pre and post analyte recognition. Fluorescence pH titrations were performed in buffer solution at a probe concentration of 10.0 μM in 0.2 M HEPES. As is shown in Fig. S1, neither the probe itself nor the product has strongly effect on fluorescence intensity by the pH of the mediums within the range from 4.0 to 8.8. These results imply that the probe will work well under physiological conditions (pH=7.4).

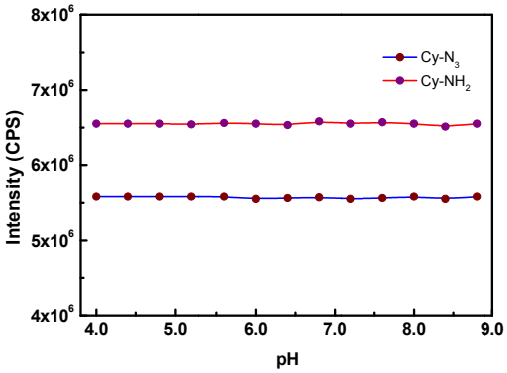

Fig. S1 Fluorescence responses of Cy-N_3 (10.0 μM) to various pH in 0.2 M HEPES. pH: 4.0, 4.4, 4.8, 5.2, 5.6, 6.0, 6.4, 6.8, 7.2, 7.6, 8.0, 8.4, 8.8. Red line: Cy-N_3 only; Blue line: Cy-NH_2.

4. Bright-Field Images of Fig. 4

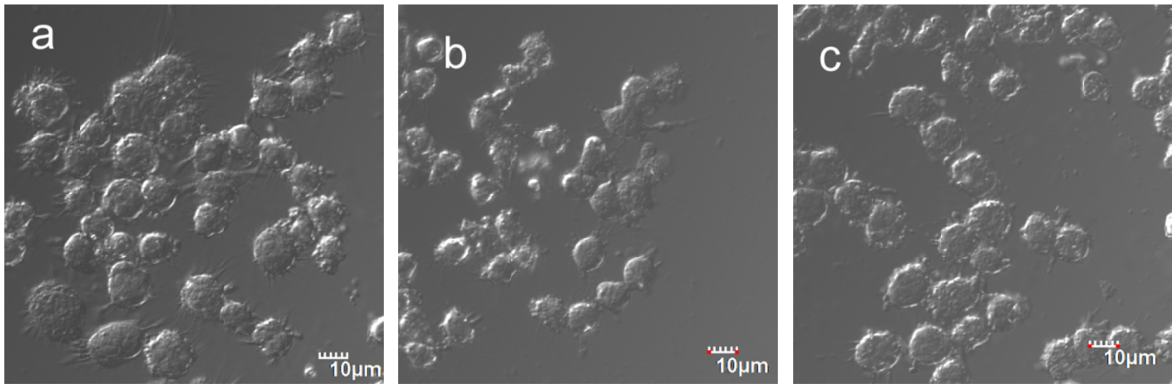

Fig. S2 Brightfield images of cells in Fig. 4. (a) Brightfield images of Fig. 4a. (b) Brightfield images of Fig. 4b. (c) Brightfield images of Fig. 4c.

5. Confocal Microscopy Imaging for Subcellular Locations of Cy-N_3 in RAW264.7 Cells

Subcellular locations of DA-Cy were investigated by costained with a nuclear counterstain SYTO-16 dye. The cell-permeant green fluorescent nucleic acid stain could exhibit bright, green fluorescence upon binding to nucleic acids (Figure S3c). Merged images of brightfield Figure S3h, Figure S3b red channel, and co-staining with SYTO-16 dye (Figure S3c) revealed the location of the probe in the cytoplasm of these living RAW264.7 cells (Figure S3g). Brightfield transmission images confirmed that the cells were still viable after these redox cycling events (Figure S3h).

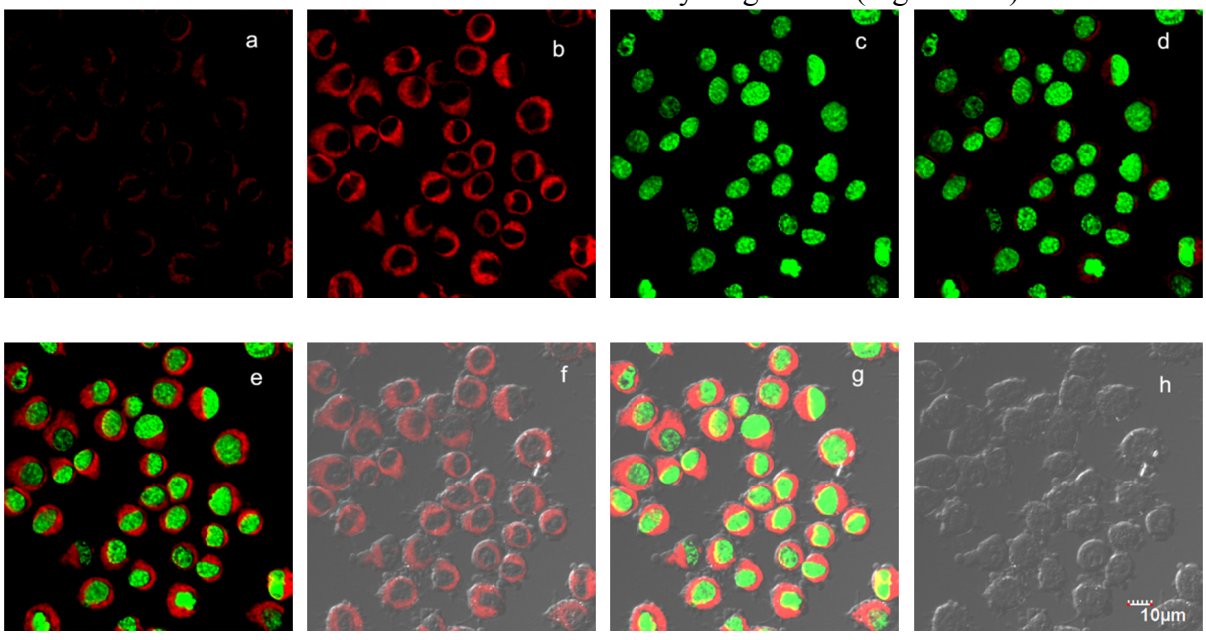

Fig. S3 Confocal microscopy imaging for subcellular locations of Cy-N_3 in living RAW264.7 macrophage cells. RAW264.7 cells incubated with 100 μM NaHS for 30 min at 37 °C with 10 μM Cy-N_3 added for the final 20 min. Fluorescence was acquired on a confocal laser-scanning microscope with excitation wavelength was 635 nm. a) Fluorescence collection windows from 650 to 712 nm. b) Fluorescence collection windows from 725 to 800 nm. c) Co-staining with 0.1 μM

SYTO-16 dye images. d) Merged a) and c). e) Merged b) and c). f) Merged b) and brightfield h). g) Merged b) red channel, c) green channel and brightfield h). h) Brightfield of these living RAW264.7 macrophage cells.

6. Colorimetric Determination of H_2S in Water Solution and Fetal Bovine Serum

We explored the ability of the probe to determine H_2S in water solution and fetal bovine serum by colorimetric method. To evaluate the capability of Cy-N_3 in the determination of H_2S concentration, the probe was treated with H_2S under varies concentrations. The final concentration of Cy-N_3 was maintained at 10 μM, while the concentrations of H_2S varied from 0 to 100 μM. As shown in Fig. S4, the absorption was linearly related to the concentration of H_2S in the given concentration range. The regression equation was $A = 0.474 \times [H_2S]\ \mu M + 0.008$, with $r = 0.996$. Next, we used fetal bovine serum to investigate whether the probe functions well in complex systems. We prepared fetal bovine serum which contained H_2S at different concentrations (0 - 100 μM). Using the same method, we got another standard curve between ratio emission intensity and H_2S concentration. The regression equation was $A = 0.544 \times [H_2S]\ \mu M + 0.007$, with $r = 0.997$. These results revealed that Cy-N_3 could test H_2S in complex biological systems both qualitatively and quantitatively. Absorption was measured at 660 nm.

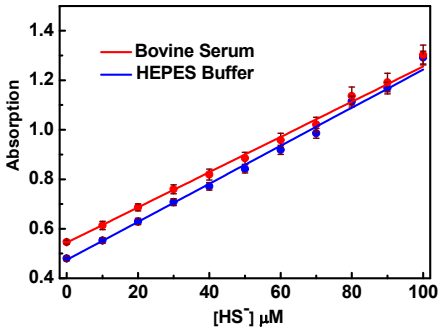

Fig. S4 The relationship between absorption and H_2S concentration in water solution (blue) and commercial fetal bovine serum (red). 10 μM Cy-N_3, 0 – 100 μM NaHS. Absorption was measured at 660 nm.

7. Time Dependent H_2S Release Associated with Decomposition of H_2S Donor ADT-OH

ADT-OH (5-(4-hydroxyphenyl)-3H-1,2-dithiol-3-thione) was chosen as the tested model. We performed parallel-controlled trials in fetal bovine serum at 37 ^oC (40 mM HEPES pH 7.4). One sample contained 500 μM ADT-OH, and the other was mixed with 100 μM NaHS as a control. The final concentration of probe was all fixed at 10 μM. As shown in Fig. S5, Cy-N_3 could respond to the released H_2S which was decomposed by H_2S donor. Absorption was measured at 660 nm.

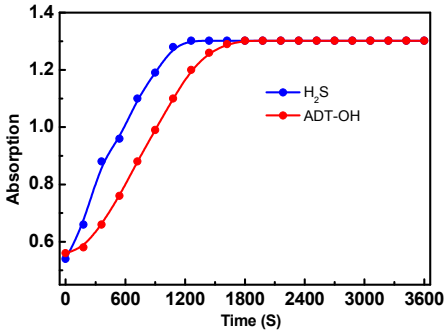

Fig. S5 Time course of reactions of 10 μM Cy-N_3 with100 μM NaHS (red) and 500 μM ADT-OH (blue). Trials were carried out in fetal bovine serum at 37 ^{o}C 40 mMHEPES pH 7.4 Absorption was measured at 660 nm.

8. RAW264.7 Cells Intracellular Free Extracts Analysis

For the preparation of intracellular cell-free extracts, cell pellets were washed twice with normal saline and resuspended in 1 mL normal saline followed by ultrasonic disruption. Sonication was performed for five 1-min intervals in an ice bath. Cell debris was removed by centrifugation at 10,000 rpm for 15 min at 4 ^{o}C, and the supernatant was the intracellular cell-free extract. Total cell numbers were adjusted to 10^9 CFU/mL for the preparation of intracellular cell-free extracts.[3] The intracellular cell-free extracts were measured by colorimetric and ratiometric fluorescence test, respectively. The experimental study includes 3 parallel control groups. First group, RAW264.7 cells were treated with PMA (1 μg/mL) for 30 min at 37 ^{o}C. Second, the control culture RAW264.7 cells. Third group, cells were incubated with 100 μM NaHS for 30 min. After ultrasonic disruption, spectroscopic experiments with Cy-N_3 were performed at 10 μM. Absorption was measured at 660 nm. Ratiometric fluorescence ($F_{750\ nm}/F_{710\ nm}$) test was excited at 625 nm. The results revealed that Cy-N_3 could test H_2S changes in RAW264.7 cells intracellular free extracts qualitatively.

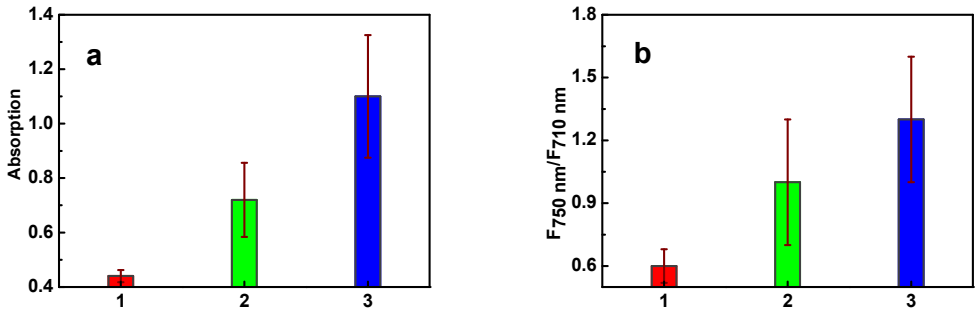

Fig. S6 Colorimetric and ratiometric fluorescence test for intracellular free extracts analysis. a) The colorimetric determination of H_2S in RAW264.7 cells intracellular free extracts. Cy-N_3 were at 10 μM, λ_{abs} = 660 nm. 1) RAW264.7 cells were treated with PMA (1 μg/mL) for 30 min at 37 ^{o}C. 2) The control culture RAW264.7 cells. 3) Cells were incubated with 100 μM NaHS for 30 min; b) Ratiometric fluorescence test for H_2S in RAW264.7 cells intracellular free extracts. Cy-N_3 were at 10 μM, Ratiometric fluorescence ($F_{750\ nm}/F_{710\ nm}$) was excited at 625 nm. 1) RAW264.7 cells were

treated with PMA (1 μg/mL) for 30 min at 37 °C. 2) The control culture RAW264.7 cells. 3) Cells were incubated with 100 μM NaHS for 30 min.

[3] Z. R. Wang, J. P. Sheng, X. L. Tian, T. T. Wu, W. Z. Liu, L. Shen, *African Journal of Microbiology Research*, 2011, 5, 4980-4986.

9. Limit of Detection

Limit of detection in analysis.[4] The limit of detection, expressed as the concentration c_L, or the quantity q_L, is derived from the smallest measure x_L, that can be detected with reasonable certainty for a given analytical procedure. The value of x_L is given by the equation:

$$x_L = \bar{x}_{bi} + k\, s_{bi} \quad (1)$$

Where $\bar{x}_{bi}$ is the mean of the blank measures, s_{bi} is the standard deviation of the blank measures, and k is a numerical factor chosen according to the confidence level desired.

$$c_L = \frac{(x_L - \bar{x}_B)}{m} \quad (2)$$

Where, m is the slope of the linear regression equation.
Combine two of the equations, Long and Winefordner defined c_L:

$$c_L = \frac{(k \cdot s_B)}{m} \quad (3)$$

Generally, κ=3, P < 0.01, we obtained c_L = 0.08 μM.

[4] IUPAC. Compendium of Chemical Terminology, 2nd ed. (the "Gold Book"). Compiled by A. D. McNaught and A. Wilkinson. Blackwell Scientific Publications, Oxford (1997). XML on-line corrected version: http://goldbook.iupac.org (2006) created by M. Nic, J. Jirat, B. Kosata; updates compiled by A. Jenkins. ISBN 0-9678550-9-8.

10. Photophysical Properties and Analysis Performances of H_2S Fluorescent Probes

Table S1. Photophysical properties and analysis performances of H_2S fluorescent probes

	Fluorophore	C_{probe}	λ_{ex}	λ_{em}	Response	Selectivity	C_{H_2S}	r^a	Φ
Cy-N_3	Cyanine	10 μM	625 nm [b]	750 nm	20 min	High	0 - 100 μM	0.995	0.12
[1] SF1	Rhodamine	10 μM	490 nm	525 nm	60 min	Moderate	Test at 100 μM	--	0.51
[1] SF2	Rhodamine	10 μM	492 nm	525 nm	60 min	High	Test at 100 μM	--	0.60
[2] DNS-Az	Dansyl chloride	200 μM	360 nm	528 nm	Seconds	High	0 - 140 μM	0.998	- [c]
[3] SFP-1	Triarylpyrazoline	10 μM	300 nm	391 nm	60 min	High	0 -50 μM	- [d]	- [e]
[3] SFP-2	BODIPY	5 μM	465 nm	510 nm	20 min	High	0 -100 μM	--	0.208
[4] FL-DS	Fluorescein	100 μM	465 nm	- [f]	60 min	High	0 -10 μM	- [g]	0.392

[5] Cyclen-AF+Cu^{2+}	Fluorescein	1 μM	491 nm	516 nm	Seconds	High	Test at 10 μM	--	-[h]
[5] TACN-AF+Cu^{2+}	Fluorescein	1 μM	492 nm	517 nm	Seconds	low	Test at 10 μM	--	0.85
[5] Cyclam-AF+Cu^{2+}	Fluorescein	1 μM	492 nm	516 nm	60 min	High	Test at 100 μM	--	0.83
[5]TMCyclen-AF+Cu^{2+}	Fluorescein	1 μM	491 nm	516 nm	60 min	High	Test at 100 μM	--	0.78
[5] DPA-AF+Cu^{2+}	Fluorescein	1 μM	491 nm	516 nm	Seconds	low	Test at 10 μM	--	0.79

[a] r = Linear Regression Coefficients

[b] absorption peak shift from 610 nm to 660 nm with isosbestic point at 625 nm

[c] 100 μM DNS-Az, 25 μM H_2S led to a 40-fold enhancement

[d] Na_2S (10 – 50 μM) fluorescence increased linearly, but r not given

[e] > 10-fold increase in the fluorescence intensity

[f] not given, generally fluorescein derivatives' λ_{em} = ~ 520 nm

[g] NaHS (0 – 10 μM) fluorescence increased linearly, but r not given

[h] increment of fluorescence intensity by 50-fold

1. A. R. Lippert, E. J. New and C. J. Chang, *J. Am. Chem. Soc.*, 2011, **133**, 10078.
2. H. Peng, Y. Cheng, C. Dai, A. L. King, B. L. Predmore, D. J. Lefer, and B. Wang, *Angew. Chem. Int. Ed.*, 2011, **50**, 9672.
3. Y. Qian, J. Karpus, O. Kabil, S. Y. Zhang, H. L. Zhu, R. Banerjee, J. Zhao, and C. He, *Nat. Commun.*, 2011, **11**,495.
4. C. Liu, J. Pan, S. Li, Y. Zhao, L. Y. Wu, C. E. Berkman, A. R. Whorton, and M. Xian, *Angew. Chem. Int. Ed.*, 2011, **50**, 10327. FL-DS was renamed by Yu Fabiao, in order to present neat.
5. K. Sasakura, K. Hanaoka, N. Shibuya, Y. Mikami, Y. Kimura, T. Komatsu, T. Ueno, T. Terai, H. Kimura, and T. Nagano, *J. Am. Chem. Soc*., 2011, **133**, 18003.

11. Theoretical and Computational Methods

[5] The Gaussian 09 package refer toGaussian 09, Revision A.02, M. J. Frisch, G. W. Trucks, H. B. Schlegel, G. E. Scuseria, M. A. Robb, J. R. Cheeseman, G. Scalmani, V. Barone, B. Mennucci, G. A. Petersson, H. Nakatsuji, M. Caricato, X. Li, H. P. Hratchian, A. F. Izmaylov, J. Bloino, G. Zheng, J. L. Sonnenberg, M. Hada, M. Ehara, K. Toyota, R. Fukuda, J. Hasegawa, M. Ishida, T. Nakajima, Y. Honda, O. Kitao, H. Nakai, T. Vreven, J. A. Montgomery, Jr., J. E. Peralta, F. Ogliaro, M. Bearpark, J. J. Heyd, E. Brothers, K. N. Kudin, V. N. Staroverov, R. Kobayashi, J. Nor-mand, K. Raghavachari, A. Rendell, J. C. Burant, S. S. Iyengar, J. Tomasi, M. Cossi, N. Rega, J. M. Millam, M. Klene, J. E. Knox, J. B. Cross, V. Bakken, C. Adamo, J. Jaramillo, R. Gomperts, R. E. Stratmann, O. Yazyev, A. J. Austin, R. Cammi, C. Pomelli, J. W. Ochterski, R. L. Martin, K. Morokuma, V. G. Zakrzewski, G. A. Voth, P. Salvador, J. J. Dannenberg, S. Dapprich, A. D. Daniels, O. Farkas, J. B. Foresman, J. V. Ortiz, J. Cioslowski, and D. J. Fox, Gaussian, Inc., Wallingford CT, 2009.

The ICT mechanism was confirmed via time-dependent density functional theory (TD-DFT) method with TZVP basis sets. Molecular excitation energies, oscillator strengths (*f*) and electron transitions were listed in Table S1 using conductor like screening solvent model (COSMO) for water. Amino, the strong electron-donor in Cy-NH_2, would decrease the LUMO energy. The smaller energy gap could induce bath chromic spectral shifts in contrast to the molecule Cy-N_3 which was decorated with a more electron-withdrawing azido group. Fig. S7 displayed that both of the molecules showed the main transition assigned to $S_0 \rightarrow S_1$ from HOMO to LUMO with the largest $f \approx 2.3$. Moreover, the

electrons in HOMO for the two molecules were delocalized over the conjugated chain of cyanine. With respect to Cy-N_3, the electrons in LUMO exhibits large overlap with those in HOMO to result in localized state (LE), and consequently triggering strong fluorescenceemission. TowardsCy-NH_2, the compound exhibited the LE state over the conjugated chain of cyanineincluding the electron transition between π-orbital of cyanine moiety and lone-electron pair of amino group. These calculations were consistent with theexperimental results and rationalize the ICT process. In order to provide further demonstration forthe molecular electron transition in the two compounds, the electron density difference maps (EDDMs) of the main states has been calculated using Gauss-Sum2.2.5 software package. The EDDMs obtained the same results as TD-DFT to reveal the ICT mechanism (Fig. S8).

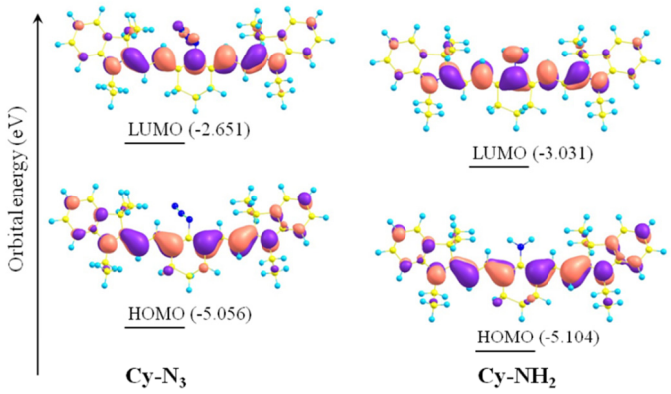

Fig. S7 Frontier molecular orbitalsand corresponding energies (unit: eV) for compounds Cy-N_3 and Cy-NH_2.

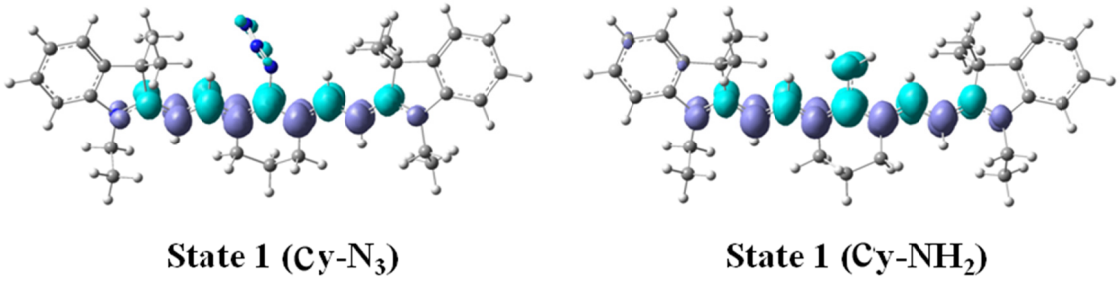

Fig. S8 Illuminated the EDDMs for the first excited state of Cy-NH_2 and Cy-N_3. The purple mark showed the electrons decreasing, and the blue region pointed the electron increasing.

Computational method:

Density functional theory (DFT) and time-dependent density functional theory (TD-DFT) methods have been carries out to study the ground state structure and electron transition for compounds Cy-N_3 and Cy-NH_2, and the latter method has been confirmed to be an effective candidate to carry out the electron transition. Herein, the Becke's three–parameter hybrid exchange functional with Lee-Yang-Parr gradient-corrected correlation (B3LYP functional)[1] has been used with the triple-ζ valence quality with one set of polarization functions (TZVP)[2] to be an

appropriate basis set for such ionic organic compounds.[3] The geometries for Cy-N_3 and Cy-NH_2 were fully optimized without symmetry constraints, and all the local minima were confirmed by the absence of an imaginary mode in vibrational analysis calculations. To clarify the origins of electron transition, the electron density difference maps (EDDMs) of the main states were calculated using Gauss-Sum2.2.5 software package.[4] An EDDM is a representation of the changes in electron density that occur for a given electronic transition.

[1] a) A. D. Becke, *J. Chem. Phys.***1993**, *98*, 5648-5652; b) P. A. M. Dirac, *Proc. Royal Soc. (London) A***1929**, *123*, 714-733; c) S. H. Vosko, L. Wilk, M. Nusair, *Can. J. Phys.***1980**, *58*, 1200-1211; d) A. D. Becke, *Phys. Rev. A***1988**, *38*, 3098-3100; e) C. Lee, W. Yang, R. G. Parr, Phys. Rev. B **1988**, *37*, 785-789.
[2] O. Treutler, R.Ahlrichs, *J. Chem. Phys.***1995**, *102*, 346 -354.
[3] S. K. Schneider, G. R. Julius, C. Loschen, H. G. Raubenheimer, G. Frenking, W. A. Herrmann, *Dalton Trans*. **2006**, 1226-1233.
[4] N. M. O'Boyle, A. L. Tenderholt, K. M. Langner, *J. Comp. Chem.***2008**, *29*, 839-845.

Calculated electronic transitions energies

Table S2. Calculated electronic transitions energies for **Cy-N_3** and **Cy-NH_2** at TD-DFT/B3LYP/TZVP level with COSMO solvation model

Compound	Transitions	λ_{cal} (nm)	λ_{exp} (nm)	*f*	CI expansion coefficients
Cy-N_3	S_0–S_1	623	611	2.3593	0.710 (HOMO → LUMO)
Cy-NH_2	S_0–S_1	572	654	2.2095	0.707 (HOMO → LUMO)

XYZ Coordinates (angstrom) and SCF Energies (a.u.)

Cy-N_3
Energy = -1593.7870089

C	-0.143565	7.502652	-2.389004
C	-0.207863	6.644965	-1.305281
C	-0.517880	7.141441	-0.041480
C	-0.763425	8.490125	0.185044
C	-0.693509	9.346948	-0.914566
C	-0.388836	8.864735	-2.186743
C	0.002690	5.145296	-1.216986
C	-0.222145	4.897517	0.284503
N	-0.533092	6.075796	0.880326
C	-0.817727	6.273965	2.305982
C	1.438387	4.780984	-1.654709
C	-1.048381	4.411724	-2.080735
C	-0.587155	-7.428670	-2.398424
C	-0.311062	-6.596916	-1.327876
C	-0.125467	-7.134881	-0.056562
C	-0.213600	-8.499711	0.189766
C	-0.493393	-9.329724	-0.896951

C	-0.678454	-8.806439	-2.175929
C	-0.146189	-5.090701	-1.263804
C	0.131319	-4.881028	0.234562
N	0.150951	-6.091192	0.848611
C	0.388408	-6.329827	2.276704
C	-1.444286	-4.388033	-1.717021
C	1.058783	-4.656324	-2.129483
C	0.332632	-3.693283	0.929578
C	0.348519	-2.408597	0.381005
C	-0.140400	3.703567	0.993993
H	0.092842	7.130749	-3.378852
H	-0.995199	8.875433	1.168652
H	-0.878372	10.404439	-0.771084
H	-0.340208	9.549711	-3.024035
H	-1.514265	7.107899	2.377445
H	-1.343162	5.394130	2.672616
H	2.176147	5.280486	-1.025024
H	1.613239	3.707004	-1.607789
H	1.590046	5.104553	-2.685556
H	-2.060269	4.666548	-1.762128
H	-0.930434	3.330396	-2.026139
H	-0.928650	4.715384	-3.121802
H	-0.731487	-7.024371	-3.393267
H	-0.079519	-8.915843	1.178909
H	-0.569389	-10.398346	-0.737763
H	-0.895638	-9.471250	-3.002664
H	1.105406	-5.590300	2.628419
H	0.873173	-7.301277	2.360977
H	-2.285865	-4.682179	-1.088080
H	-1.348510	-3.303686	-1.681935
H	-1.666478	-4.675064	-2.745984
H	1.219390	-3.580253	-2.086765
H	1.971927	-5.155450	-1.801688
H	0.869466	-4.931761	-3.168087
H	0.477187	-3.779829	1.996756
C	0.475622	-1.227419	1.114358
C	0.149244	2.451566	0.450794
H	0.199750	-2.315652	-0.684419
H	0.321502	2.378653	-0.612583
C	0.441316	0.034998	0.478208
C	0.221795	1.250458	1.159776
C	0.051258	1.187699	2.660354
C	0.541991	-1.274762	2.629051
H	0.330821	2.140999	3.108734

H	-1.003952	1.020975	2.909515
C	0.901868	0.067768	3.256047
H	-0.426387	-1.612554	3.016752
H	1.271175	-2.029561	2.934424
H	1.958759	0.288397	3.077125
H	0.761613	0.019635	4.337722
C	-0.891473	-6.293466	3.109812
C	0.436614	6.549554	3.132730
H	-0.321272	3.761317	2.057706
H	-0.646258	-6.493043	4.154448
H	-1.599959	-7.051834	2.773621
H	-1.373155	-5.316578	3.051240
H	0.152770	6.709070	4.174455
H	0.951315	7.443466	2.777497
H	1.130000	5.708462	3.091426
N	0.520997	0.133941	-0.947038
N	1.443191	-0.404063	-1.550691
N	2.238218	-0.819537	-2.235813

Cy-NH_2

Energy = -1485.5351341

C	0.476854	7.598274	-2.362450
C	0.178932	6.713224	-1.342339
C	-0.331225	7.184440	-0.133797
C	-0.549964	8.538377	0.093991
C	-0.245105	9.423456	-0.942378
C	0.261380	8.965891	-2.157410
C	0.308472	5.202140	-1.278453
C	-0.201657	4.913511	0.147863
N	-0.563005	6.098100	0.726661
C	-1.081727	6.263610	2.085769
C	1.786778	4.790191	-1.451886
C	-0.583372	4.548937	-2.357425
C	-0.461980	-7.561652	-2.438868
C	-0.200713	-6.699189	-1.389675
C	0.085172	-7.204872	-0.122871
C	0.110816	-8.570430	0.135779
C	-0.154688	-9.432408	-0.930406
C	-0.437412	-8.940744	-2.203472
C	-0.153756	-5.182916	-1.347832
C	0.182413	-4.930299	0.134421
N	0.324580	-6.135625	0.758561
C	0.642566	-6.334260	2.174389
C	-1.526909	-4.596884	-1.742067

C	0.962324	-4.663493	-2.281723
C	0.338434	-3.726712	0.797776
C	0.226566	-2.446410	0.224383
C	-0.305395	3.703469	0.804979
H	0.872712	7.242963	-3.306690
H	-0.937181	8.906916	1.034349
H	-0.405308	10.484289	-0.792610
H	0.491020	9.671576	-2.946038
H	-1.739317	7.132021	2.075556
H	-1.705683	5.402129	2.319174
H	2.411077	5.251474	-0.685021
H	1.912934	3.709598	-1.394645
H	2.141579	5.122244	-2.429170
H	-1.630357	4.819993	-2.213003
H	-0.503639	3.462534	-2.347050
H	-0.270345	4.899709	-3.342191
H	-0.683137	-7.180149	-3.428790
H	0.321530	-8.964778	1.120620
H	-0.141834	-10.501810	-0.758311
H	-0.640835	-9.629152	-3.014270
H	1.332500	-5.549156	2.480060
H	1.185363	-7.275311	2.252770
H	-2.308651	-4.947066	-1.066209
H	-1.520251	-3.507705	-1.727174
H	-1.777413	-4.919333	-2.754057
H	1.031238	-3.576461	-2.262379
H	1.931268	-5.075713	-1.995880
H	0.745751	-4.971840	-3.305845
H	0.564993	-3.778189	1.853193
C	0.331293	-1.247681	0.909052
C	0.012341	2.441279	0.263580
H	0.000599	-2.400228	-0.830745
H	0.350909	2.434496	-0.762063
C	0.217148	-0.001758	0.203328
C	-0.047994	1.222868	0.911444
C	-0.341736	1.103158	2.388840
C	0.497567	-1.256239	2.417562
H	-0.272351	2.076966	2.870715
H	-1.364013	0.741717	2.555440
C	0.649835	0.132482	3.030460
H	-0.375964	-1.746974	2.862784
H	1.358025	-1.876617	2.686347
H	1.665612	0.507620	2.871955
H	0.491145	0.077395	4.109792

C	-0.594751	-6.353548	3.070620
C	0.019279	6.438584	3.130834
H	-0.671597	3.732312	1.821073
H	-0.289765	-6.514255	4.106338
H	-1.272350	-7.159451	2.784573
H	-1.136048	-5.408138	3.015631
H	-0.432028	6.561497	4.117155
H	0.622878	7.322303	2.918336
H	0.676308	5.568213	3.160536
N	0.338590	0.009672	-1.143477
H	0.050700	0.797406	-1.698141
H	0.711280	-0.777091	-1.646278

Vibrational frequencies for compounds Cy-N_3 and Cy-NH_2.

Compound Cy-N_3

mode	wave number	IR intensity	selection rules
1	13.0634	0.0444	YES
2	13.4812	0.3975	YES
3	22.7821	0.0663	YES
4	32.4340	0.0802	YES
5	39.4196	0.0162	YES
6	47.5443	0.5757	YES
7	54.2545	0.6651	YES
8	65.6575	0.1086	YES
9	67.8097	0.3227	YES
10	73.0601	0.0587	YES
11	81.0488	3.3957	YES
12	87.4985	3.1491	YES
13	96.1285	0.3276	YES
14	100.2450	0.1632	YES
15	106.4910	0.6266	YES
16	109.8571	0.6687	YES
17	134.5530	0.6648	YES
18	139.7601	0.2591	YES
19	154.6936	0.1243	YES
20	163.7799	3.6781	YES
21	190.8863	8.1875	YES
22	204.8759	8.6444	YES
23	211.1550	1.4327	YES
24	211.9550	1.1244	YES
25	212.9980	8.0381	YES
26	220.8356	40.1030	YES
27	234.0304	1.9345	YES

28	237.0913	0.1929	YES
29	242.6395	0.3635	YES
30	244.2750	1.6213	YES
31	250.0532	0.0800	YES
32	258.4341	0.0404	YES
33	264.1045	5.9950	YES
34	272.1039	0.2537	YES
35	276.5035	2.1771	YES
36	297.7354	16.5673	YES
37	304.3564	121.0506	YES
38	310.0905	14.5746	YES
39	314.8409	40.6683	YES
40	345.4146	2.4090	YES
41	351.4455	0.2560	YES
42	355.5663	4.3433	YES
43	357.2285	4.2156	YES
44	391.6855	37.2499	YES
45	417.0252	17.2585	YES
46	425.2518	37.7634	YES
47	430.8284	12.9057	YES
48	435.8277	4.4687	YES
49	458.2458	49.7280	YES
50	472.7747	29.5187	YES
51	484.7658	9.8467	YES
52	485.2141	59.4909	YES
53	498.2021	0.2105	YES
54	516.8823	570.5885	YES
55	531.4976	0.6548	YES
56	547.0603	15.7381	YES
57	558.1070	176.2271	YES
58	558.3173	7.2118	YES
59	559.1980	24.2335	YES
60	563.3469	6.4894	YES
61	566.4108	50.3990	YES
62	576.9522	11.9633	YES
63	582.2749	13.1138	YES
64	622.6197	1.5380	YES
65	630.4319	3.3124	YES
66	644.2351	160.0849	YES
67	680.9875	15.9624	YES
68	690.3322	17.4012	YES
69	702.9358	41.8106	YES
70	707.4797	11.1151	YES
71	730.3386	566.1926	YES

72	736.6717	26.4390	YES
73	742.6686	0.0567	YES
74	743.3994	1.4610	YES
75	754.5172	139.9413	YES
76	759.8350	99.2143	YES
77	760.5184	144.6732	YES
78	781.7949	1662.8349	YES
79	789.1811	8.2552	YES
80	815.4286	519.6903	YES
81	822.7577	2.0040	YES
82	844.1714	99.0991	YES
83	849.8994	7.3844	YES
84	858.6190	658.9855	YES
85	869.5170	0.7869	YES
86	870.5063	3.2173	YES
87	873.7797	53.9343	YES
88	880.2749	65.5985	YES
89	887.7738	288.7563	YES
90	927.7509	1355.7782	YES
91	939.9985	55.8304	YES
92	941.1439	147.8666	YES
93	948.3867	2269.5511	YES
94	948.5763	145.6805	YES
95	948.5964	1.7358	YES
96	950.4224	404.5480	YES
97	952.3088	27.7786	YES
98	954.5206	44.6656	YES
99	955.8057	33.7174	YES
100	964.9359	23.0690	YES
101	968.8878	32.7828	YES
102	969.5554	6.2962	YES
103	970.2484	11.7799	YES
104	1038.5014	5315.3155	YES
105	1040.1801	26.6600	YES
106	1041.4251	22.2615	YES
107	1043.2629	247.2781	YES
108	1054.4371	163.5900	YES
109	1056.0299	3398.9476	YES
110	1063.2384	99.0986	YES
111	1069.5596	4254.5271	YES
112	1078.9512	2207.4444	YES
113	1093.5589	7486.4681	YES
114	1102.0612	5.2135	YES
115	1109.1887	2603.3556	YES

116	1111.7761	125.5929	YES
117	1118.6834	8345.4428	YES
118	1139.9548	134.5721	YES
119	1144.3878	1009.9633	YES
120	1148.9720	32.0724	YES
121	1150.7826	59.7053	YES
122	1155.4328	9.0693	YES
123	1175.0277	3018.6749	YES
124	1179.2841	35.8948	YES
125	1180.0904	155.4825	YES
126	1185.9712	4393.4311	YES
127	1196.8897	4.0992	YES
128	1199.4043	658.9351	YES
129	1234.6760	1473.6430	YES
130	1236.4257	87.4189	YES
131	1258.6151	40.6137	YES
132	1265.2772	5755.1037	YES
133	1274.9183	50.0393	YES
134	1280.3466	27.7543	YES
135	1288.9711	299.4695	YES
136	1295.3488	7.0807	YES
137	1299.5874	37.9963	YES
138	1307.6673	14.0155	YES
139	1313.1550	31.3475	YES
140	1324.3868	12.8080	YES
141	1327.3868	57.9304	YES
142	1344.8691	298.2889	YES
143	1348.5323	502.0123	YES
144	1361.4778	47.6414	YES
145	1367.6726	331.3843	YES
146	1373.7984	35.8515	YES
147	1380.6001	772.8170	YES
148	1384.3072	269.1325	YES
149	1388.2280	110.4968	YES
150	1393.8409	877.2749	YES
151	1397.0031	378.6076	YES
152	1401.8923	87.0616	YES
153	1403.1825	15.7321	YES
154	1403.8501	26.6410	YES
155	1406.4451	18.4724	YES
156	1410.5137	121.9073	YES
157	1411.0506	29.7340	YES
158	1418.9946	4041.2719	YES
159	1426.8612	106.8682	YES

160	1434.0905	29.4834	YES
161	1434.9965	24.2376	YES
162	1468.2082	577.8191	YES
163	1473.8010	17.7477	YES
164	1474.2244	0.4294	YES
165	1476.7560	5.0120	YES
166	1479.6276	6.3760	YES
167	1480.3015	23.9552	YES
168	1481.2824	2.6869	YES
169	1481.5119	2.5901	YES
170	1482.8033	169.1056	YES
171	1483.8059	7.0958	YES
172	1485.4168	361.9410	YES
173	1487.7961	83.4049	YES
174	1489.6641	7.9110	YES
175	1491.7012	56.3149	YES
176	1492.2224	36.9072	YES
177	1497.3246	20.4917	YES
178	1498.3002	10.8140	YES
179	1512.4621	128.7871	YES
180	1513.0796	63.6475	YES
181	1518.8532	459.7473	YES
182	1522.8451	35.1402	YES
183	1540.8207	1208.1056	YES
184	1550.1008	46.7034	YES
185	1578.6036	3018.7513	YES
186	1613.1401	68.3722	YES
187	1634.2907	8.2228	YES
188	1634.4718	16.5808	YES
189	1644.9680	19.7260	YES
190	1646.5906	5.8478	YES
191	2229.6957	1491.6339	YES
192	3004.3859	40.2153	YES
193	3007.7743	29.8167	YES
194	3029.7776	51.9875	YES
195	3043.2332	34.9663	YES
196	3043.4731	35.2796	YES
197	3044.2029	31.2412	YES
198	3044.4741	33.1404	YES
199	3046.9124	17.6953	YES
200	3047.3200	24.4204	YES
201	3057.6873	49.8751	YES
202	3078.4739	75.7046	YES
203	3086.9295	73.6564	YES

204	3089.0479	72.9192	YES
205	3091.5133	31.5204	YES
206	3109.1702	15.0083	YES
207	3109.3426	16.6684	YES
208	3111.3075	16.8600	YES
209	3111.5907	16.9172	YES
210	3113.0734	39.7818	YES
211	3113.2896	48.3909	YES
212	3113.7933	69.7484	YES
213	3113.8521	52.8029	YES
214	3126.1428	15.9795	YES
215	3127.0355	32.8512	YES
216	3128.5461	62.9705	YES
217	3133.1183	42.3228	YES
218	3134.1038	23.0640	YES
219	3135.5099	22.4146	YES
220	3177.9331	5.2148	YES
221	3178.2689	4.5595	YES
222	3185.5105	8.9923	YES
223	3186.1174	9.2095	YES
224	3197.2587	34.7034	YES
225	3197.4215	34.7859	YES
226	3207.4427	12.1800	YES
227	3210.1657	4.9482	YES
228	3210.5380	17.3826	YES
229	3211.1385	13.4629	YES
230	3222.5746	8.6433	YES
231	3223.4594	6.0707	YES

Compound Cy-NH_2

mode	wave number	IR intensity	selection rules
1	8.8116	0.0420	YES
2	18.4894	0.0666	YES
3	22.0461	0.0964	YES
4	35.4635	1.2344	YES
5	37.4683	0.2199	YES
6	50.0298	0.6147	YES
7	56.8981	0.4002	YES
8	65.9837	0.3633	YES
9	74.0444	0.0378	YES
10	82.7683	2.4868	YES
11	87.2834	4.1402	YES
12	91.1791	0.8835	YES
13	99.6477	0.6903	YES

14	108.6092	0.2113	YES
15	131.8372	0.8953	YES
16	135.4799	0.4532	YES
17	141.1941	2.5933	YES
18	157.6198	1.5098	YES
19	186.6808	11.8514	YES
20	200.8625	8.3791	YES
21	206.0793	44.2131	YES
22	207.7092	3.0439	YES
23	207.9081	0.8115	YES
24	223.2376	63.3588	YES
25	233.6429	159.2117	YES
26	238.1856	55.6973	YES
27	241.3169	11.7311	YES
28	242.5831	26.8985	YES
29	251.7484	107.3500	YES
30	255.3380	50.8425	YES
31	256.4450	3.8462	YES
32	258.6165	1.9250	YES
33	269.5682	11.5889	YES
34	274.7927	6.0208	YES
35	286.0750	27.4036	YES
36	305.2442	0.2723	YES
37	316.3400	222.5612	YES
38	322.4597	5.3656	YES
39	347.2967	4.0155	YES
40	350.3322	1.7934	YES
41	355.3840	1.5425	YES
42	355.7720	8.1794	YES
43	395.3490	30.2108	YES
44	415.4915	17.3938	YES
45	430.5410	4.6614	YES
46	434.7414	4.4126	YES
47	457.4806	35.8829	YES
48	467.7180	12.9432	YES
49	474.6683	2.9494	YES
50	482.1516	18.3228	YES
51	483.7645	9.2353	YES
52	502.1905	14.1338	YES
53	521.4811	22.4055	YES
54	538.5369	4.7696	YES
55	549.2353	233.7404	YES
56	556.6914	88.0788	YES
57	558.3613	32.6519	YES

58	559.0761	0.8305	YES
59	563.4874	6.3506	YES
60	574.7633	4.5269	YES
61	579.2366	7.5409	YES
62	614.0101	40.6019	YES
63	622.3734	0.7886	YES
64	643.8246	156.3537	YES
65	651.3249	12.0219	YES
66	690.9702	10.7121	YES
67	696.5647	13.9196	YES
68	699.6485	4.3905	YES
69	722.7191	144.9089	YES
70	732.6086	195.8348	YES
71	740.2955	0.5441	YES
72	740.9602	1.0777	YES
73	749.4151	9.6690	YES
74	757.3727	122.6058	YES
75	758.8431	131.8017	YES
76	780.1301	1103.3325	YES
77	787.5796	16.8346	YES
78	811.1021	329.1084	YES
79	821.0826	2.8333	YES
80	841.9449	5.2627	YES
81	849.3901	15.8609	YES
82	855.9442	233.4992	YES
83	865.4682	1.2166	YES
84	866.8435	12.0340	YES
85	867.5223	54.8072	YES
86	881.0352	204.4030	YES
87	885.6881	615.6495	YES
88	915.0959	265.6987	YES
89	935.6712	151.5780	YES
90	939.3694	535.2425	YES
91	940.2175	34.0866	YES
92	940.9048	154.4738	YES
93	946.4961	2.4570	YES
94	946.8803	7.3151	YES
95	949.6854	311.5819	YES
96	951.4677	46.2528	YES
97	953.5112	11.7826	YES
98	954.8359	1.3413	YES
99	965.5384	0.2773	YES
100	967.4436	0.7934	YES
101	986.3207	134.8572	YES

102	1035.3771	7.7246	YES
103	1040.8943	1531.4081	YES
104	1042.8464	1.3675	YES
105	1043.1747	9.8944	YES
106	1056.2358	578.7767	YES
107	1061.8107	59.7564	YES
108	1067.8307	398.6239	YES
109	1075.2654	1892.5037	YES
110	1094.2209	6024.5243	YES
111	1100.7511	6.7381	YES
112	1103.1118	1145.6316	YES
113	1109.2148	12.9742	YES
114	1112.7997	898.0015	YES
115	1137.7066	158.6366	YES
116	1139.7939	203.9054	YES
117	1149.3746	1709.9663	YES
118	1151.0303	70.5530	YES
119	1152.4682	142.6335	YES
120	1153.3989	12.1988	YES
121	1165.0470	28.8307	YES
122	1178.7375	368.1860	YES
123	1179.2353	51.3525	YES
124	1190.3359	640.8952	YES
125	1197.5692	509.5486	YES
126	1198.8110	6391.1843	YES
127	1199.0552	370.2071	YES
128	1235.0045	727.7997	YES
129	1238.7850	509.6373	YES
130	1271.4681	2591.8708	YES
131	1275.8883	147.9949	YES
132	1276.4860	199.7510	YES
133	1281.4856	26.7369	YES
134	1292.7775	3.6911	YES
135	1298.8944	2877.2369	YES
136	1309.1827	261.5706	YES
137	1309.8091	123.9334	YES
138	1315.9842	68.2395	YES
139	1325.0511	22.6434	YES
140	1334.9344	1087.1663	YES
141	1351.5377	261.1330	YES
142	1357.9460	17.5173	YES
143	1365.4345	368.0118	YES
144	1376.1786	15.6536	YES
145	1384.0506	769.2880	YES

146	1388.9685	19.0244	YES
147	1389.3755	96.4879	YES
148	1397.4548	365.6861	YES
149	1398.8217	5.9935	YES
150	1400.0187	528.7961	YES
151	1400.9965	142.1768	YES
152	1403.4683	11.2402	YES
153	1406.1716	30.3860	YES
154	1407.5774	364.7474	YES
155	1410.3859	3005.0397	YES
156	1410.5332	75.4081	YES
157	1428.9470	50.7155	YES
158	1433.5686	136.6670	YES
159	1461.2786	17.4618	YES
160	1473.5498	0.9943	YES
161	1475.4617	394.0574	YES
162	1476.0004	28.8553	YES
163	1479.3690	1.5124	YES
164	1480.1247	8.2387	YES
165	1480.8585	24.3540	YES
166	1481.3351	11.4986	YES
167	1481.3789	32.0602	YES
168	1483.7547	143.5171	YES
169	1484.3135	3.3345	YES
170	1484.8724	263.7182	YES
171	1487.5080	158.4962	YES
172	1489.2828	39.2387	YES
173	1491.6529	54.8166	YES
174	1494.0025	116.2421	YES
175	1496.2167	34.5044	YES
176	1498.1315	10.8108	YES
177	1513.5661	50.7403	YES
178	1513.9054	47.0556	YES
179	1516.6945	116.8910	YES
180	1519.7114	145.9072	YES
181	1554.9623	2349.9251	YES
182	1566.8861	813.1296	YES
183	1582.8685	2625.8323	YES
184	1617.7772	79.5368	YES
185	1634.7140	25.2237	YES
186	1634.7967	18.8042	YES
187	1643.9738	44.6970	YES
188	1646.3441	16.3347	YES
189	1654.3058	256.5217	YES

190	3001.6301	61.6547	YES
191	3003.3961	17.8218	YES
192	3024.8664	34.5341	YES
193	3040.9584	78.8331	YES
194	3041.5666	33.6858	YES
195	3041.8029	49.4884	YES
196	3041.8562	20.1202	YES
197	3042.0365	37.0466	YES
198	3044.9121	7.6348	YES
199	3044.9867	25.5214	YES
200	3071.8241	91.0113	YES
201	3081.5645	58.0055	YES
202	3083.8583	55.0727	YES
203	3104.5714	31.7177	YES
204	3105.6751	8.6499	YES
205	3106.7105	11.7226	YES
206	3109.0601	16.2929	YES
207	3109.8062	16.1734	YES
208	3110.7699	53.9964	YES
209	3110.8576	51.9532	YES
210	3111.5362	52.9445	YES
211	3111.6564	50.8698	YES
212	3121.3236	7.6203	YES
213	3122.1288	16.2044	YES
214	3123.3120	82.3406	YES
215	3124.5255	73.4700	YES
216	3128.6222	35.8526	YES
217	3130.6843	31.8785	YES
218	3175.7762	4.0755	YES
219	3176.3677	3.4856	YES
220	3182.8990	11.6595	YES
221	3183.6494	10.7282	YES
222	3195.6330	31.6581	YES
223	3195.9396	30.5232	YES
224	3202.3920	11.5860	YES
225	3202.6376	0.2972	YES
226	3206.7006	13.9364	YES
227	3206.8424	12.5840	YES
228	3214.2241	18.9085	YES
229	3218.2508	19.0113	YES
230	3603.9988	113.3521	YES
231	3714.1381	86.9443	YES